

# EVALUATION OF THE THORACIC DEFLECTION MEASUREMENT SYSTEM 'RIBEYE' IN THE HYBRID III 50% IN FRONTAL SLED TESTS

Andre Eggers

Thorsten Adolph

Federal Highway Research Institute, BASt  
Germany

Paper Number 11-0190

## ABSTRACT

Thoracic injury is one of the predominant types of severe injuries in frontal accidents. The assessment of the injury risk to the thorax in the current frontal impact test procedures is based on the uni-axial chest deflection measured in the dummy Hybrid III. Several studies have shown that criteria based on the linear chest potentiometer are not sensitive enough to distinguish between different restraint systems, and cannot indicate asymmetric chest loading, which has been shown to correlate to increased injury risk. Furthermore, the measurement is sensitive to belt position on the dummy chest. The objective of this study was to evaluate the optical multipoint chest deflection measurement system 'RibEye' in frontal impact sled tests. Therefore the sensitivity of the RibEye system to different restraint system parameters was investigated. Furthermore, the issue of signal drop out at the 6<sup>th</sup> rib was investigated in this study. A series of sled tests were conducted with the RibEye system in the Hybrid III 50%. The sled environment consisted of a rigid seat and a standard production three-point seat belt system. Rib deflections were recorded with the RibEye system and additionally with the standard chest potentiometer. The tests were carried out at crash pulses of two different velocities (30 km/h and 64 km/h).

The tests were conducted with different belt routing to investigate the sensitivity of chest deflection measurements to belt position on the dummy chest. Furthermore, different restraint system parameters were investigated (force limiter level, with or without pretensioning) to evaluate if the RibEye measurements provide additional information to distinguish between restraint system configurations. The results showed that with the RibEye system it was possible to identify the effect of belt routing in more detail.

The chest deflections measured with the standard chest potentiometer as well as the maximum deflection measured by RibEye allowed the distinction to be made between different force limiter levels.

The RibEye system was also able to clearly show the asymmetric deflection of the rib cage due to belt loading. In some configurations, differences of more than 15 mm were observed between the left

and side areas of the chest. Furthermore, the abdomen insert was identified as source of the problem of signal drop out at the 6<sup>th</sup> rib. Possible solutions are discussed.

In conclusion, the RibEye system provided valuable additional information regarding the assessment of restraint systems. It has the potential to enable the evaluation of thoracic injury risk due to asymmetric loading.

Further investigations with the RibEye should be extended to tests in a vehicle environment, which include a vehicle seat and other restraint system components such as an airbag.

## INTRODUCTION

Studies of accident data show that a high portion of severe and fatal injuries in motor vehicle accidents occur in frontal impacts even without intrusion in the passenger compartment. The mainly injured body part is the thorax (Carroll et al. 2010).

The assessment of the injury risk to the thorax in the current frontal impact test procedures is based on the uni-axial chest deflection measured in the dummy Hybrid III. Several studies have shown that criteria based on the linear chest potentiometer are not sensitive enough to distinguish between different restraint systems Petitjean et al. (2002), and cannot indicate asymmetric chest loading, which has been shown to correlate to increased injury risk (Shaw et al. 2009).

The RibEye system (Handman, 2007) allows multipoint measurements of chest deflection in the dummy Hybrid III 50%. With these additional deflection measurements it could be possible to obtain more detail of the location of highest deflection on the dummy chest and also capture the effect of asymmetric loading. If it would be possible to measure this asymmetrical deflection it could be a basis for improved chest injury risk criteria based on the Hybrid III.

The accuracy of the RibEye system was evaluated in quasi-static indenter tests and dynamic pendulum tests by Yogandan et al. (2009a, 2009b). The RibEye system installed in the dummy Hybrid III 5% female was evaluated by Tylko et al. (2007) in full scale crash tests. However, no systematic sled tests with the RibEye system have been reported so far.

Another multi-point chest deflection measurement system called THMPR (Thorax Multi-Point and high Rate measurement device) based on IR-Tracc installed in the Hybrid III was evaluated in sled tests by Petitjean (2002, 2003). It was found that with this type of multi-point deflection measurement it is possible to identify the point of highest deflection, which is not always the sternum. It was also reported that with this device it was possible to identify asymmetric chest deflection due to belt loading.

The objective of this study was a systematic evaluation of RibEye system installed in the Hybrid III 50% to investigate if it is also possible with this system to capture asymmetric loading, and achieve a higher sensitivity of possible criteria based on RibEye deflection measurement with respect to restraint system parameters.

## METHODOLOGY

A series of 13 frontal impact sled tests were conducted with the dummy Hybrid III. The sled environment consisted of a rigid seat, a foot rest and a standard production three-point seat belt system.

### Sled Test Setup And Restraint System

To be able to conduct a high number of tests in a repeatable test setup, a generic rigid seat and foot rest was used, which was available from sled tests completed under the European project FID (Frontal Impact Dummy). The same seat geometry was also used for tests at INRETS by Vezin and tests at BAST under the FID project, as reported in Vezin et al. (2002). The geometry of the seat, and the foot rest geometry is shown in Figure 1 and Figure 2.

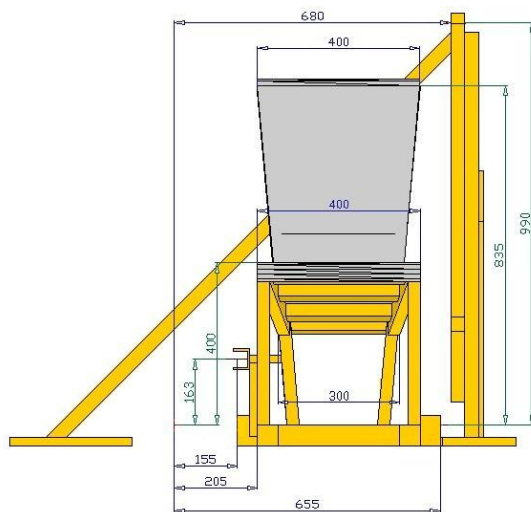


**Figure 1. Front view of the seat geometry with dimensions.**

For the test series a standard production three-point seat belt system was used, which consisted of a pretensioner and retractor. The belt geometry represents a midsize European vehicle. The belt attachment points were based on data collected from several European cars and published by Zellmer et al. (1998). The attachment points with respect to the dummy H-points are given in Table 1. The test setup is shown in Figure 3.

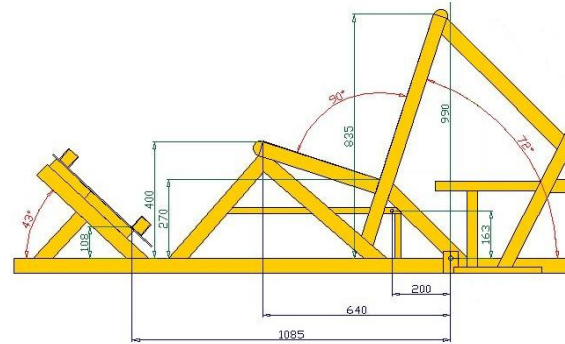


**Figure 2. Lateral view of the seat and foot rest geometry with dimensions.**

**Table 1. Belt attachment points, which were used for all sled test in this test series**

| Belt point w.r.t Dummy H-point | X (mm) | Y (mm) | Z (mm) |
|--------------------------------|--------|--------|--------|
| Retractor                      | -150   | -301   | -216   |
| Buckle                         | -191   | 233    | -194   |
| D-ring                         | -316   | -284   | 606    |
| Anchor                         | -316   | -284   | -462   |



**Figure 3. The test setup consisted of a rigid seat, foot rest and a standard three-point belt system.**

### Instrumentation

The dummy was instrumented according to the standard requirements for the Euro NCAP frontal impact tests (Euro NCAP, 2009). Additionally, the rib deflection was measured at 12 points with the RibEye system. An overview of all measured

dummy data channels is given in Table 2. The dummy was equipped with a neck shield for all of the tests to avoid interaction between the belt and neck.

Additionally, the sled deceleration pulse and the belt forces at the shoulder and the lap belt force at the anchor were recorded. All data was filtered according to SAE J211 where applicable. The filter classes are also shown Table 2.

**Table 2.**  
**Instrumentation of the Hybrid III for the frontal sled tests according to standard Euro NCAP frontal impact instrumentation and additionally 2-axis, 12 point RibEye system**

| Segment | Parameter   | CFC  |
|---------|---|------|
| Head    | Acceleration ( $a_{x,y,z}$ )                                    | 1000 |
| Neck    | Upper forces ( $F_{x,y,z}$ )                                    | 1000 |
|         | Upper moments ( $M_{x,y,z}$ )                                   | 600  |
| Chest   | Deflection ( $\delta_x$ )                                       | 180  |
|         | Acceleration ( $a_{x,y,z}$ )                                    | 180  |
|         | RibEye deflection ( $\delta_{x,y}$ )                            | 600  |
| Pelvis  | Acceleration ( $a_{x,y,z}$ )                                    | 1000 |
| Femur   | Femoral left and right load ( $F_z$ )                           | 600  |
| Tibia   | Tibia left and right upper loads ( $F_{x,z}$ )<br>$M_{x,y,z}$ ) | 600  |
|         | Tibia left and right upper loads ( $F_{x,z}$ )<br>$M_{x,y,z}$ ) | 600  |
| Knee    | Knee slider left and right ( $\delta_x$ )                       | 180  |

### RibEye Configuration

In addition to the standard Euro NCAP Hybrid III instrumentation shown in Table 2 (including the chest potentiometer), the dummy was equipped with the standard 2D RibEye system (Handman, 2007), which is able to measure the rib deflection in x and y directions at each of the six ribs located left and right of the sternum. A detailed description of the system is provided in earlier publications (Yoganadan, 2009a). The RibEye used in this study consists of 12 LEDs, which can be placed on arbitrary position along the ribs. In a study by Yoganandan et al. (2009b) the optimal LED position for this system was determined to be at 9 cm measured along the outer curvature of the rib (Figure 4). In this study, those LED positions were used for all tests.

### Dummy Positioning

The Hybrid III dummy was positioned on the seat with the back against the back rest and the thighs on the seat. The feet were positioned flat on the foot rests. The H-point of the dummy was moved to the position as specified in Table 1. The distance between the knees was adjusted to 150 mm. The pelvis angle was set to  $22.5^\circ \pm 2.5^\circ$  and the head angle between  $0^\circ$  and  $2^\circ$ .

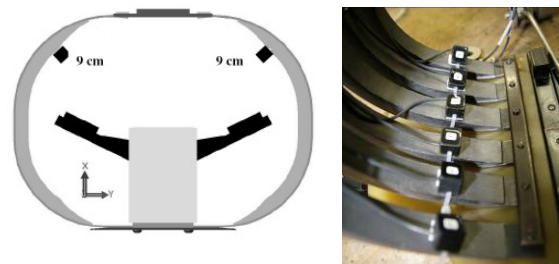


**Figure 4.** Attachment position of the LEDs at 9 cm measured from the centre of the sternum along the outer curvilinear path of the rib.

### High Speed Film Cameras

Three digital high-speed fixed position cameras recording 1,000 frames per second were used to capture one lateral view, one top view and one frontal view.

### Test Parameters

Within the test series several parameters including the impact severity and restraint system parameters were varied to investigate their influence on the deflection output measured by the RibEye and the standard chest potentiometer. The belt system, including retractor buckle and the belt itself were changed after each test.

**Crash Pulse** Two different crash pulses were applied; a 30 km/h pulse, required as per ECE regulation R44 (shown in Figure 5), and a 64 km/h Euro NCAP frontal ODB crash pulse of a midsize vehicle (shown in Figure 6).

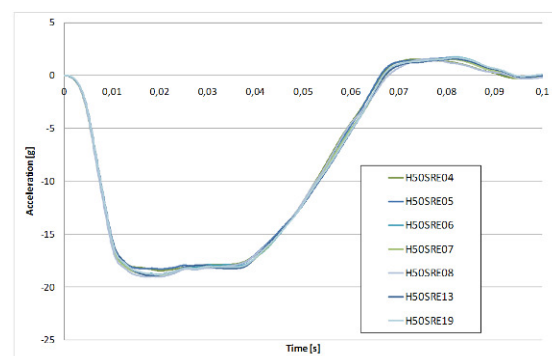


**Figure 5.** 30 km/h sled pulse (R44-03 regulation)

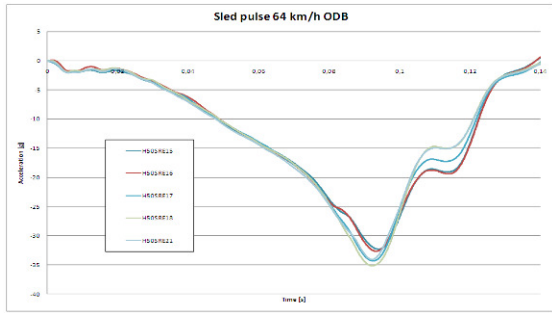


**Figure 6. 64 km/h ODB Euro NCAP frontal sled pulse.**

**Pretensioner** The belt retractor used in the tests was equipped with a pretensioner which was fired 17 ms after impact in some tests depending on the test configuration.

**Load Limiter** Two different load limiter levels were used. One load limiter had a torsion bar of 95 mm to get a high shoulder belt force. To achieve the desired belt force a residual lap of 640 mm was used on the spool for all tests with this load limiter. To achieve a lower shoulder belt force, a load limiter with a torsion bar of 42 mm diameter was used. For all tests with this load limiter, a residual lap of 475 mm was used to obtain the desired force at the shoulder belt.

**Belt Routing On Dummy Chest** The belt was positioned in two different ways. ‘Normal’ and ‘High’ positions were defined as follows. For the ‘Normal’ belt position the belt was routed in a way that it was just below the right of the two holes, which are part of the dummy chest flesh jacket (left photo in Figure 7). In the ‘High’ belt position the belt is touching the neck shield (right photo in Figure 7).

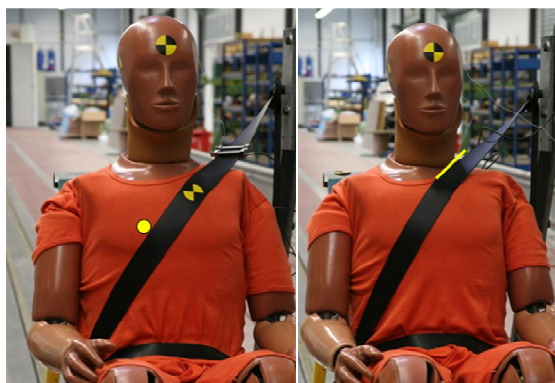


**Figure 7. Normal belt position (left) and high belt position (right).**

To investigate if the RibEye system is able to distinguish between different restraint systems and furthermore to evaluate the sensitivity to belt position a matrix of 10 configurations was defined

(Table 3.). Some tests configurations were repeated; resulting in a total number of 13 tests.

**Table 3. Combination of test parameters**

| Variations | Impact velocity [km/h] | Belt routing | Load limiter level | Belt pretensioner |
|------------|------------------------|--------------|--------------------|-------------------|
| 1          | 30                     | Normal       | Low                | No                |
| 2          |                        |              | Low                | Yes               |
| 3          |                        |              | High               | No                |
| 4          |                        |              | High               | Yes               |
| 5          |                        | High         | Low                | Yes               |
| 6          |                        |              | High               | No                |
| 7          | 64                     | Normal       | Low                | Yes               |
| 8          |                        |              | High               | No                |
| 9          |                        | High         | Low                | Yes               |
| 10         |                        |              | High               | Yes               |

### Additional Tests To Investigate Signal Dropout At The 6<sup>th</sup> Rib

To investigate the signal drop out at the 6<sup>th</sup> rib which was frequently observed within this test series and was also reported by other researchers (Tylco et al. 2007) additional tests were performed. Four tests additional to the described test matrix were performed with a camera capturing the view inside the dummy chest. To achieve this, the head and neck of the dummy was removed, and an aluminum block was mounted to the neck support of the dummy. A high speed camera facing towards the chest interior was attached to the block (Figure 8).



**Figure 8. A camera facing down into the inside of the chest of the dummy**

The objective of this was to investigate possible interaction between the abdomen and LEDs attached to the 6<sup>th</sup> rib.

To ensure the chest flesh of the jacket would not obstruct the camera view during belt-induced

compression of the chest, part of the jacket was cut away in the required area. To have enough light available in the chest cavity of the dummy to enable high speed filming, three LED bands with a light intensity of 330 lumen each (Figure 9) were attached to the spine box of the dummy.

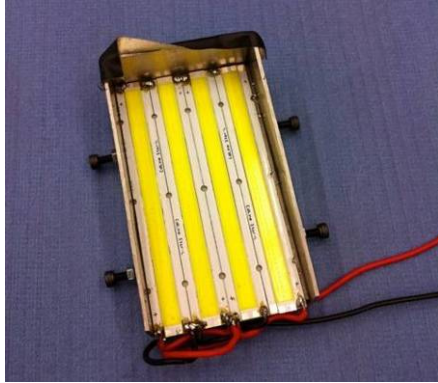


**Figure 9. Four LEDs were attached to the spine box to illuminate the inside of the chest for high speed filming**

In the tests with this additional camera it was not possible to record useful RibEye data during the tests. Due to the high illumination inside the chest, which was necessary for high speed filming, the optical sensors of the RibEye system were not able to record the light emitted by the RibEye LEDs.

In addition to these tests, one test was performed with the standard Hybrid III dummy equipped with RibEye, but without abdomen insert, to investigate if the signal drop out problem is eliminated in the case of the absence of the abdomen insert.

## RESULTS

Table 4 shows a matrix of successful tests conducted within this test series, indicating the test parameters and corresponding test number.

**Table 4. Configurations of the 13 tests to investigate the influence of tests parameters on output signals of the RibEye system**

| Test No. | v [km/h] | Load limiter | Belt routing | Pretensioner |
|----------|----------|--------------|--------------|--------------|
| H50SRE04 | 30       | High         | Normal       | No           |
| H50SRE05 | 30       | Low          | Normal       | No           |
| H50SRE06 | 30       | Low          | Normal       | Yes          |
| H50SRE07 | 30       | High         | Normal       | Yes          |
| H50SRE08 | 30       | High         | High         | No           |
| H50SRE13 | 30       | Low          | High         | Yes          |
| H50SRE15 | 64       | Low          | High         | Yes          |
| H50SRE16 | 64       | High         | High         | Yes          |
| H50SRE17 | 64       | High         | Normal       | No           |
| H50SRE18 | 64       | Low          | High         | Yes          |
| H50SRE19 | 30       | Low          | High         | Yes          |
| H50SRE20 | 30       | Low          | High         | Yes          |
| H50SRE21 | 64       | Low          | Normal       | Yes          |

Selected dummy sensor and belt force characteristic peak values from the 13 tests are shown in Table 5. For tests with high velocity and low load limiter level (15, 17, 21) the chest of the dummy contacted the femur during the forward movement of the chest. This happened after the belt-induced maximum chest deflection was reached. This ‘first deflection’ maximum due to belt loading is given in the table and is used for further analysis. A similar approach was used to determine the relevant peak values for the deflections measured by the RibEye system.

**Table 5. Characteristic result values of the 13 sled tests**

| Test No. | Peak Head Acceleration Resultant [g] | Peak Chest Deflection [mm] | Peak Upper diagonal Belt Force [kN] | Peak Pelvis Acceleration Resultant [g] |
|----------|--------------------------------------|----------------------------|-------------------------------------|--|
| H50SRE04 | 38.1                                 | 30.3                       | 6.5                                 | 33.4                                   |
| H50SRE05 | 26.6                                 | 21.2                       | 3.4                                 | 36.0                                   |
| H50SRE06 | 22.2                                 | 20.5                       | 4.5                                 | 28.0                                   |
| H50SRE07 | 31.0                                 | 29.2                       | 6.4                                 | 28.6                                   |
| H50SRE08 | 38.1                                 | 26.0                       | 6.3                                 | 37.2                                   |
| H50SRE13 | 22.5                                 | 19.6                       | 3.8                                 | 28.4                                   |
| H50SRE15 | 42.5                                 | 25.9                       | 4.4                                 | 37.7                                   |
| H50SRE16 | 40.3                                 | 30.7                       | 7.6                                 | 42.6                                   |
| H50SRE17 | 48.8                                 | 34.9                       | 7.4                                 | 60.7                                   |
| H50SRE18 | 46.7                                 | 24.1                       | 5.1                                 | 50.1                                   |
| H50SRE19 | 22.5                                 | 18.8                       | 3.7                                 | 30.6                                   |
| H50SRE20 | 22.5                                 | 21.2                       | 3.6                                 | 29.0                                   |
| H50SRE21 | 43.9                                 | 24.3                       | 4.7                                 | 41.3                                   |

The highest chest deflection of 34.9 mm was observed in the configuration 64km/h, without pretensioner, high load limiter and normal belt position. The lowest chest deflection of 19.6 mm occurred in the configuration 30 km/h, with pretensioner fired, low load limiter level and high belt position.

In the following figures plots are shown of the RibEye outputs measured in the test H50SRE04 with an impact velocity of 30 km/h, high load limiter, normal belt routing and pretensioner not fired. The seat belt forces are also plotted for this test in Figure 10. The displacements of the ribs in x-direction and the left and right side are shown in Figure 11 and Figure 12.

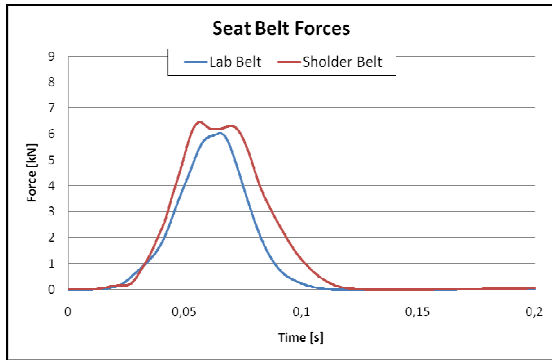


**Figure 10. Seat belt forces in test H50SRE04**

An effect can be observed in these figures which occurred in all tests reported here. The signal at the 6<sup>th</sup> rib is interrupted at both sides of the rib cage. At the right rib this occurs after the maximum deflection was already reached (Figure 11). At the left 6<sup>th</sup> rib the signal drops out at 55 ms and comes back at 200 ms. This problem can occur when the light path from the LED to one or both of the optical receivers is interrupted. The reason for this could be parts inside the dummy (such as the rod of the chest potentiometer), blocking the light path, or high deformations of the ribs, which cause the LED to move out of the range of sight of the optical sensors. The hypothesis also stated by other researchers who observed signal drop out at the 6<sup>th</sup> rib is interference with the abdomen insert, which moves up during the forward movement of the dummy and interacts with the LED or blocks the light path. This issue was investigated by additional tests within this study and is described later.

The highest rib deflections measured with the RibEye occurred at the right half of the rib cage at the 1<sup>st</sup> rib, 25.5 mm (Figure 11). This was observed in all tests reported in this test series. The reason could be that the shoulder takes most of the load at the retractor side, which shields the ribs. This leads to higher deflection at the buckle side.

The deflection measured at the 1<sup>st</sup> right rib is lower compared to the peak deflection measured with the chest potentiometer (30.3 mm). The peak deflection measured with the RibEye LED configuration used in this study was lower than the deflection measured by the chest potentiometer. Of course, this is dependent on the locations where the LEDs are attached to the ribs. The 9 cm position used in this study is quite far away from the center of the sternum. An LED position closer to the sternum (or even sternum-mounted LEDs), could result in deflections measured by RibEye which are higher than the peak deflections measured by the chest potentiometer.

Comparing the right and left x-deflection (Figure 11 and Figure 12) it can be noted that the deflections at the right side of the chest (the buckle side) are higher than the deflection at the retractor side. This was the case for all tests in this test series. The difference of left and right x-deflection was

calculated for all tests. For test H50SRE04 it is plotted in Figure 13. The peak difference calculated from this plot is quite high compared to the peak deflection itself, which is 11.0 mm for this test configuration. This shows that with the RibEye installed in the Hybrid III chest it is possible to capture asymmetric deflection due to belt loading.

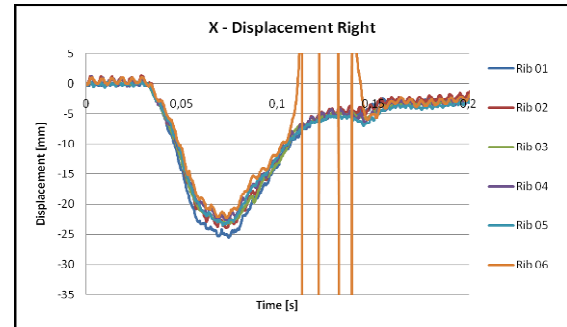


**Figure 11. x-displacements of right ribs 1 to 6 in test H50SRE04**

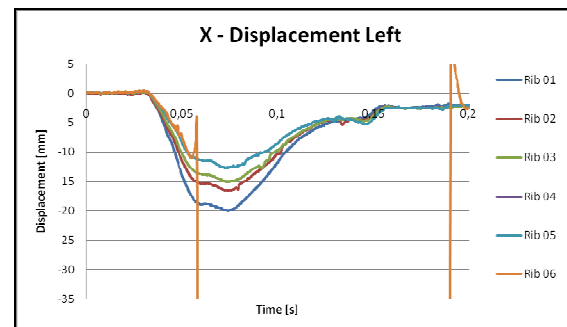


**Figure 12. x-displacements of left ribs 1 to 6 in test H50SRE04**

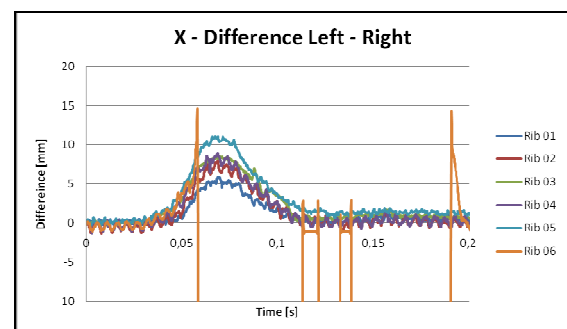


**Figure 13. Deflection difference calculated between left and right for test H50SRE04**

The y-displacements left and right for this test configuration are plotted in Figure 14 and Figure 15. The same signal drop out effect like for the x-deflection can be observed in these plots for the signals of the 6<sup>th</sup> rib. The peak y-displacements at the right ribs are notably high for this test configuration. The highest peak deflection of 12.5 mm was observed at the 1<sup>st</sup> right rib. The y-deflections at the right ribs were higher for all test configurations.

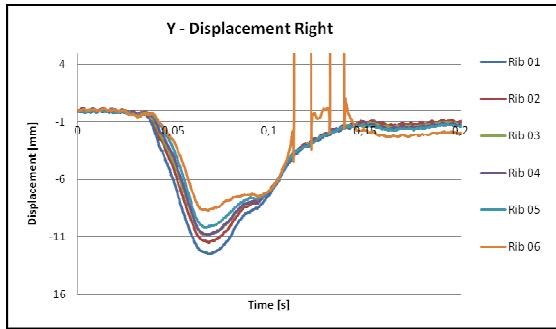


**Figure 14. y-displacements of right ribs 1 to 6 in test H50SRE04**

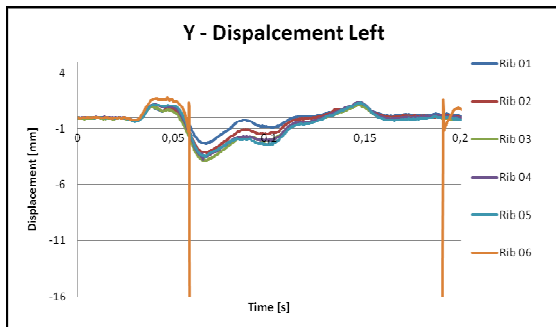


**Figure 15. y-displacements of left ribs 1 to 6 in test H50SRE04**

Plots of RibEye sensor data outputs from other test configurations are omitted from this paper, for brevity. However, all relevant signals were evaluated; characteristic peak values were calculated and are summarized in Table 6. The deflection measured by the chest potentiometer is also given in this table for comparison. The

maximum x-deflection measured by RibEye (which was always observed in at the 1<sup>st</sup> right rib), is also shown, along with the difference between peak deflection measured by the chest potentiometer and RibEye for each test, which was up to 7 mm in some tests.

The difference between deflection measured at the right and left side of the rib cage was calculated to understand the influence of test parameters on asymmetrical chest deflection. The values given in the table are not the difference of peak deflections at the left and right side. To obtain values for the right and left deflection, curves were subtracted for all rib levels respectively to obtain difference curves for each rib (see Figure 13 for example plot). Table 6 shows the peak value of the curve with the maximum difference between left and right. The next column in Table 6 indicates the rib level where the highest peak difference was observed, which was rib level 5 for most tests. Only in two cases the highest peak deflection occurred at rib level 3.

The maximum difference between left and right was 16.3 mm for the test configuration 64 km/h, high belt load limit, high belt position, with pretensioner fired. The lowest difference of 4.9 mm was observed in the test configuration 64 km/h, low load limiter level, normal belt routing, with pretensioner.

**Table 6  
Rib deflection values measured and calculated based on RibEye output**

| Testno.  | Peak Deflection from Chest Potentiometer | Maximum x-deflection (at Rib1Right) | Difference Rib1Right to Chest Potentiometer | Maximum Difference Left - Right | Rib Level of Maximum Left-Right Difference | Maximum y-deflection (at Rib1Right) |
|----------|--|-------------------------------------|---|---------------------------------|--|-------------------------------------|
| H50SRE04 | 30.3                                     | 25.5                                | 4.9   | 11.0                            | 5  | 12.5                                |
| H50SRE05 | 21.2                                     | 17.9                                | 3.3   | 7.1                             | 5  | 9.5                                 |
| H50SRE06 | 20.5                                     | 16.3                                | 4.2   | 5.1                             | 5  | 8.7                                 |
| H50SRE07 | 29.2                                     | 24.9                                | 4.3   | 10.4                            | 5  | 10.8                                |
| H50SRE08 | 26.0                                     | 25.1                                | 0.9   | 14.8                            | 5  | 7.7                                 |
| H50SRE13 | 19.6                                     | 17.4                                | 2.2   | 6.9                             | 5  | 6.7                                 |
| H50SRE15 | 25.9                                     | 23.9                                | 2.0   | 9.5                             | 3  | 6.9                                 |
| H50SRE16 | 30.7                                     | 29.0                                | 1.7   | 16.3                            | 5  | 7.4                                 |
| H50SRE17 | 34.9                                     | 27.9                                | 7.0   | 12.6                            | 5  | 15.2                                |
| H50SRE18 | 24.1                                     | 21.8                                | 2.3   | 8.5                             | 5  | 7.9                                 |
| H50SRE19 | 18.8                                     | 17.4                                | 1.4   | 6.6                             | 5  | 6.5                                 |
| H50SRE20 | 21.2                                     | 19.2                                | 2.0   | 7.7                             | 3  | 6.0                                 |
| H50SRE21 | 24.3                                     | 20.0                                | 4.4   | 4.9                             | 5  | 9.9                                 |

## Sensitivity Of Chest Deflection Values To Restraint Parameters

One main objective of the study was to investigate a correlation of test parameters (Table 4) and deflection values measured by chest pot and RibEye (Table 6). For the parameters; ‘load limiter level’ and ‘belt routing’ on the chest of the dummy, correlations to deflection parameters were found and are presented here.

Figure 16 shows the 13 tests performed with this test series, sorted from left to right in descending order by peak chest deflection measured by the chest potentiometer. The results show that the highest deflection occurs in the five tests with high load limiter level. In all tests with the lower load limiter level the deflection measured by the chest potentiometer is lower. This observation suggests that based on the tests conducted within this study, a criterion based on chest deflection measured by the chest potentiometer is able to show the positive effect of a load limiter.

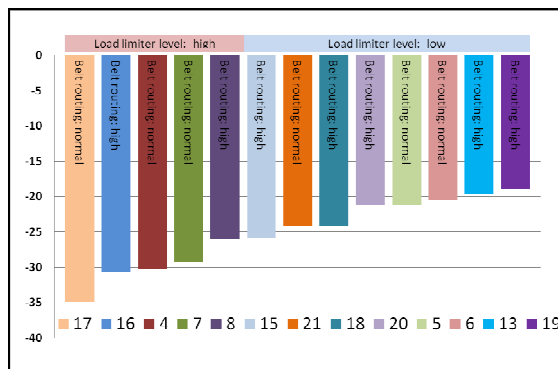


**Figure 16. Peak chest deflections in mm measured by chest potentiometer**

Figure 17 shows the peak x-deflection measured at the 1<sup>st</sup> right rib by RibEye sorted in descending order. The same effect as in Figure 16 is demonstrated. High deflection corresponds to test configurations with high load limiter level. Lower deflection values at the 1<sup>st</sup> right rib can be observed in tests with a lower load limiter level. This implies that peak deflection measured by RibEye in Hybrid III is also a parameter which can show the difference between different load limiter levels.

In both figures the belt routing is also indicated within the bars of the diagrams. Comparing this in Figure 16 and Figure 17 shows that the order of some adjacent bars (representing tests with high and low belt routing), is switched. For example, tests 16 and 17, tests 7 and 8, tests 21 and 18. This implies that both peak chest deflection measured by the chest potentiometer and RibEye are able to show the effect between different shoulder belt loads, but are both sensitive to belt position. The deflection measured by the chest potentiometer is higher for the normal belt position whereas the

maximum deflection value measured by RibEye is higher for the high belt position.

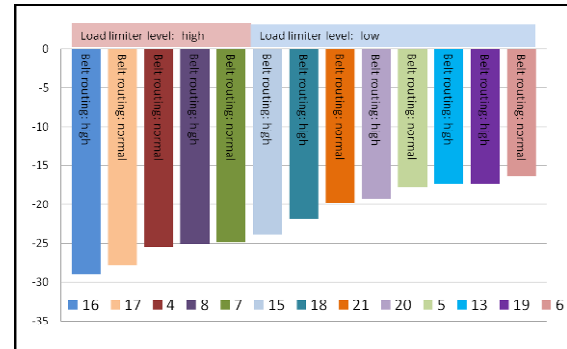


**Figure 17. Peak x-deflection in mm measured by RibEye at 1<sup>st</sup> right rib**

The effect of belt routing on the difference between peak deflection measured by the chest potentiometer and RibEye can be further understood by looking at Figure 18, which shows the tests sorted by this difference in descending order. It shows that the difference is higher for the 6 tests with normal belt routing. If the belt is moved to a higher position on the chest of the dummy, the deflection at the chest potentiometer decreases, whereas the deflection measured at the 1<sup>st</sup> right rib increase at the same time. This leads to a lower difference between the two measurements.

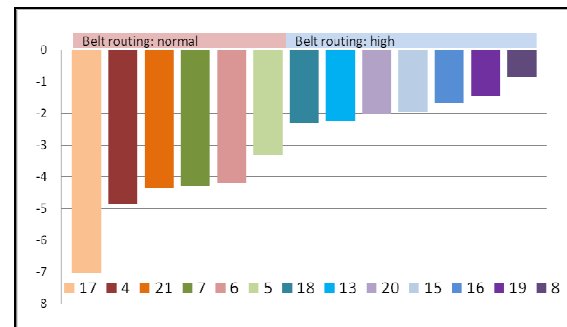


**Figure 18. Difference in mm between peak chest deflection measured by chest potentiometer and RibEye**

Figure 19 shows the peak difference of left at right deflection measured by RibEye, which occurred at rib level 5 for most test configurations. The graph shows that this parameter is higher in the five test configurations with high load limiter level. For the tests with low shoulder belt load this difference is lower. This result suggests that an assessment criterion based on the difference between right and left deflection would also be able to show the positive effect of a load limiter.

The last deflection parameter, which was considered in this sensitivity analysis, is the peak y-deflection, which was observed at the 1<sup>st</sup> right rib for all tests within this test series. The test configurations sorted in descending order by y-



deflection are presented in Figure 20. The graph shows that the peak y-deflection at the 1<sup>st</sup> right rib is sensitive to belt routing. The highest deflection values occur in tests with normal belt routing. Therefore, high belt routing appears to correlate with low y-deflection.

To illustrate the effect of parameters such as belt load level and belt routing not only on peak values on the first right rib, but also the distribution of deflection between the 1<sup>st</sup> and 6<sup>th</sup>, the resultant peak deflection values for all ribs on the left and right side of the rib cage are shown in Figure 21 and Figure 22 for selected test configurations.

In Figure 19 the peak deflection values are compared for different load limiters. Crash pulse (64 km/h), belt routing (high) and pretensioner (fired) are the same for both tests.

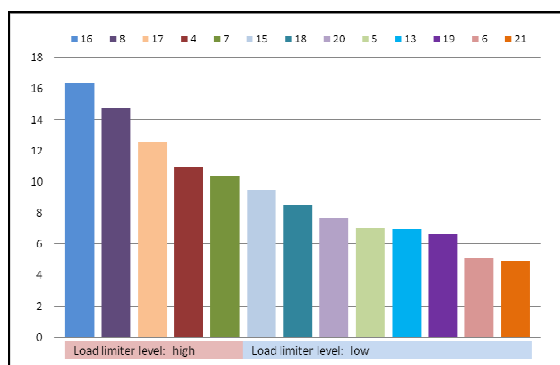


**Figure 19. Maximum difference in mm between left rib deflection and right rib deflection**

It is shown that a lower shoulder belt force results in a reduction of deflections measured by the chest potentiometer and the RibEye LEDs on the right part of the chest. For the left ribs only small reduction of deflection can be observed for the

upper ribs. The lower ribs sustain a very small increase in deflection for the lower belt load.

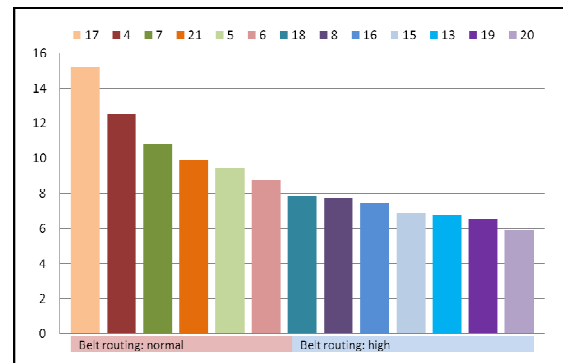


**Figure 20. Maximum y-deflection in mm at 1<sup>st</sup> right rib**

In Figure 22 the chest deflections are shown for two tests to compare the effect of belt routing. The other parameters 'sled pulse' (30 km/h), 'load limiter' (low) and 'pretensioner' (fired) were not changed between the two configurations. As previously explained, the figure shows that the deflection measured by the chest potentiometer is reduced for higher belt position on the chest of the dummy whereas the peak deflection measured by the RibEye 1<sup>st</sup> right rib increases.

It is shown that this is also true for the deflection at the right side of the chest down to the 4<sup>th</sup> rib. However, at the left side of the chest the deflection is decreased for a higher belt routing. This could be also due to the shielding effect of the shoulder as described before.

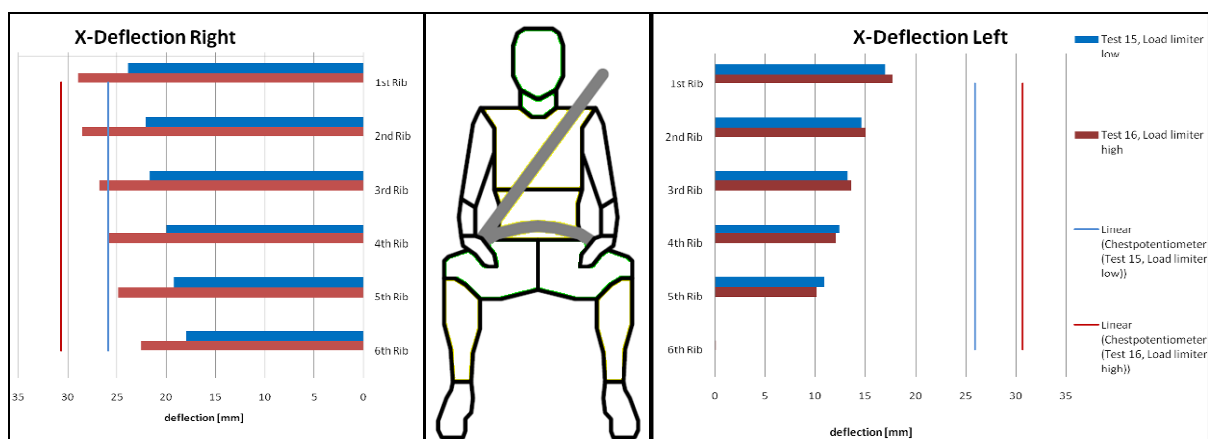


**Figure 21. Peak chest deflection measured by chest potentiometer (straight line), peak deflections at ribs 1 to 6 left and right (bar graphs) compared for two tests with different load limiter.**

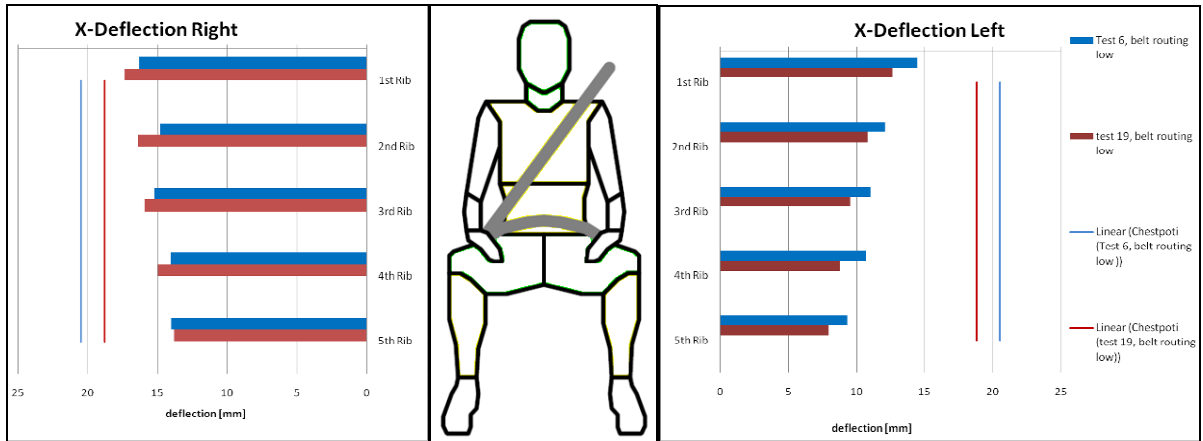


**Figure 22. Peak chest deflection measured by chest potentiometer (straight line), peak deflection at ribs 1 to 6 left and right (bar graphs) compared for two tests with different belt routing.**

### Additional Tests To Investigate Interaction Between 6<sup>th</sup> Rib And Abdomen Insert

As observed within the test series reported here and also described by other researchers, signal dropout occurred at the LEDs attached to the 6<sup>th</sup> rib. The hypothesis stated by other researchers was that this effect could be a result of interaction between LEDs on the 6<sup>th</sup> rib and the abdomen insert. This was investigated by additional sled tests with a camera viewing inside the chest cavity of the

dummy. The 30 km/h sled pulse and a low belt load limiter were used in these tests. A diagram of one of the tests is shown in Figure 23. The left figure shows the dummy on the sled 46 ms after impact. The right figure shows an image captured by the high speed video inside the chest cavity. In this photo it is possible to see reflections of the red light emitted by the LED on the 6<sup>th</sup> left rib (highlighted by the green box). This explains the signal drop out which occurred in several tests on the 6<sup>th</sup> rib.

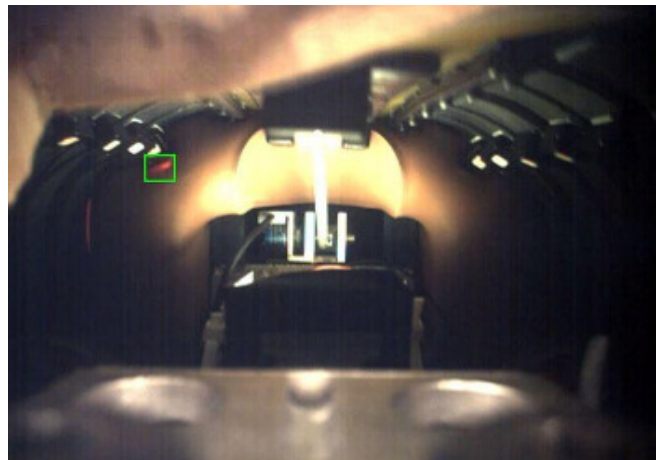


**Figure 23. Dummy with camera mounted on neck viewing into the chest of Hybrid III at 46 ms during sled test (left photo). Screen shot of camera view inside dummy chest at 46 ms (right photo); reflection of RibEye LED-light (highlighted by green box) indicating abdomen insert blocking the light path.**

To support this finding, one additional test was conducted without the abdomen insert. The configuration of the test was 64 km/h, low load limiter, high belt routing and the pretensioner was fired. In this test no signal dropout occurred, which is a further indication that the signal dropout observed in the other tests is caused by the abdomen insert.

Displacement signals measured by RibEye for this test are shown in Figure 24 and Figure 25.

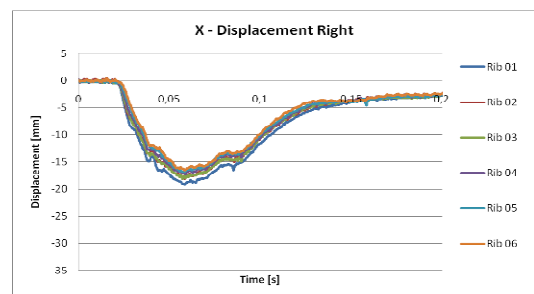


**Figure 24. Deflections measured by RibEye at rib1 to rib6 right in test without abdomen insert**

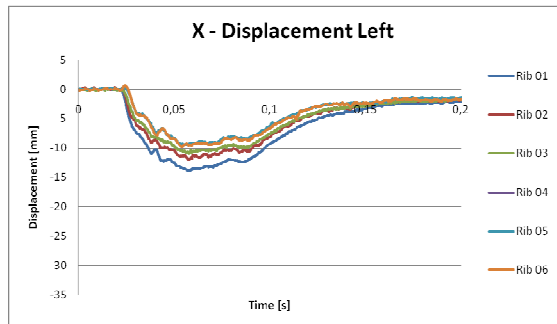


**Figure 25. Deflections measured by RibEye at rib1 to rib6 left in test without abdomen insert**

## CONCLUSIONS AND RECOMMENDATIONS

This study aimed to systematically evaluate the possible benefit of additional deflection outputs measured by the RibEye installed in the dummy Hybrid III in a series of thirteen sled tests.

It was demonstrated that based on the peak chest deflection measured by the standard chest potentiometer as well as peak deflection measured by the RibEye on the 1<sup>st</sup> right rib, it was possible to distinguish between configurations with high and low belt load limiter level. Furthermore, it was shown that the peak deflection detected by the chest potentiometer is sensitive to the initial belt position on the chest of the dummy. The maximum peak deflection measured by RibEye, which always occurred at the 1<sup>st</sup> right rib is also sensitive to belt routing, but as the RibEye measures the deflection at multiple points, this effect can be better understood by reviewing the change of deflection due to different belt routing on both sides of the chest.

By considering the peak difference between left and right deflection it was also possible to distinguish between tests with high and low load limiters. The analysis of the peak difference between left and right chest deflection showed that the RibEye installed in the rib cage of Hybrid III is able to indicate asymmetric loading (as shown by Petitjean) even though the chest is very stiff compared to more biofidelic frontal impact dummies such as THOR. This implies that it would be worthwhile to investigate possible injury criteria, taking into account the right to left difference in chest deflection measurements of the Hybrid III.

A further objective of this study was to investigate the problem of signal drop out at the 6<sup>th</sup> rib. The dummy abdomen insert was identified as a source of interference. If the RibEye should be used in tests procedures to assess the effectiveness of restraint systems based on a criterion which takes into account measurements from the 6<sup>th</sup> rib, a solution to this issue is required.

One possibility could be to try different LED positions. For example, LEDs placed at a position 12 cm from the sternum center line would be out of

the interaction area with the abdomen insert. However, at this position they might be out of the regular range of sight of the RibEye system. Another possibility could be a modification of the abdomen. However, this would change the behavior of the entire dummy and should be avoided. A third possibility could be to change the design of the LED cases, which are presently relatively large, and thus offer a high area for interaction with the abdomen insert.

## Limitation Of The Study And Further Research

This study was completed in a rigid lab seat environment with a belt system only. It should be extended to a sled environment, which more closely represents a vehicle, including a vehicle seat as well as state of the art restraint systems such as airbags, knee bolsters, or knee airbags.

Furthermore, it is recommended to investigate other LED configurations including LEDs closer to the sternum or sternum mounted LEDs. It would also be of interest to use other presently available RibEye systems which also allow for measurement of z-displacement of the ribs.

## REFERENCES

Carroll, Jolyon; Adolph, Thorsten; Chauvel, Cyril. 2010. "Overview of serious thorax injuries in european frontal car crash accidents and implications for crash test dummy development." Proceeding of the IRCOBI conference 2010, Hannover.

EUROPEAN NEW CAR ASSESSMENT PROGRAMME (Euro NCAP). 2009. "FRONTAL IMPACT TESTING PROTOCOL, Version 5.0". [www.euroncap.com](http://www.euroncap.com)

Handman, D.F.. Multipoint position measuring and recording system for anthropomorphic test devices. 2007. Boxboro systems. LLC. Newton. NA: USA.

Kent, R. Lessley, D.; Shaw, G.; Crandall, J. 2003. "The Utility of Hybrid III and THOR Chest Deflection for Discriminating Between Standard and Force-Limiting Belt Systems". Stapp Car Crash Journal, 47, pp. 267–297.

Petitjean, A.; Lebarbe, M.; Potier, P.; Trosseille, X.; Lassau, J.-P. 2002. "Laboratory Reconstructions of Real World Frontal Crash Configurations using the Hybrid III and THOR Dummies and PMHS". Stapp car crash journal, 46, pp. 27–54.

Petitjean, A.; Baudrit, P.; Trosseille, X. 2003. "Thoracic injury criterion for frontal crash

applicable to all restraint systems". " Stapp Car Crash Journal. 47. pp. 323–348.

Rouhana S. Elhagediab A. Chapp J. (1998) A High-speed Sensor for Measuring Chest Deflection in Crash Test Dummies. Proc. Sixteenth Enhanced Safety of Vehicles. pp. 2017–2045.

Tylko. S.; Charlebois. D.; Bussièrès. A. 2007."Comparison of Kinematic and Thoracic Response of the 5th Percentile Hybrid III in 40, 48 and 56 km/h Rigid Barrier Tests". Paper Number 07-0506. Technical Conference on the Enhanced Safety of Vehicles.

Veizin. P.; Bruyere-Garnier. K.; Bermond. F.; Verriest. J. P. 2002. "Comparison of Hybrid III. Thor-alpha and PMHS Response in Frontal Sled Tests. " Stapp car crash journal. 46. pp. 1–26.

Yoganandan. N.; Pintar. F. A. 2009a. "Evaluation of the Ribeye Deflection Measurement System". Paper number 09-0020. Technical Conference on the Enhanced Safety of Vehicles.

Yoganandan. N.; Pintar. F. A. 2009b. "Optimal Sensor Positioning to Track Rib Deflections from an Optical System in the Hybrid III Dummy". " Traffic Injury Prevention. 10. pp. 497–505.

Zellmer. H.; Brüggemann. K.; Lührs. S. 1998."Optimierte Rückhaltesysteme für Fondinsassen - Advanced Restraint Systems for Rear Seat Occupants". BAG & BELT '98. Cologne.